

ARGO-YBJ constraints on very high energy emission from GRBs

The ARGO-YBJ Collaboration:

G. Aielli ^{a,b}, C. Bacci ^{c,d}, B. Bartoli ^{e,f}, P. Bernardini ^{g,h},
 X.J. Bi ⁱ, C. Bleve ^{g,h}, P. Branchini ^d, A. Budano ^d, S. Bussino ^{c,d},
 A.K. Calabrese Melcarne ^x, P. Camarri ^{a,b}, Z. Cao ⁱ, A. Cappa ^{j,k},
 R. Cardarelli ^b, S. Catalanotti ^{f,e}, C. Cattaneo ^l, P. Celio ^{c,d},
 S.Z. Chen ^{i,*}, Y. Chen ⁱ, N. Cheng ⁱ, P. Creti ^h, S.W. Cui ^m,
 B.Z. Dai ^o, G. D'Alí Staiti ^{n,p}, Danzengluobu ^q, M. Dattoli ^{j,k,r},
 I. De Mitri ^{g,h}, B. D'Ettorre Piazzoli ^{f,e}, M. De Vincenzi ^{c,d},
 T. Di Girolamo ^{f,e}, X.H. Ding ^q, G. Di Sciascio ^b, C.F. Feng ^s,
 Zhaoyang Feng ⁱ, Zhenyong Feng ^t, F. Galeazzi ^d, P. Galeotti ^{j,r},
 R. Gargana ^d, Q.B. Gou ⁱ, Y.Q. Guo ⁱ, H.H. He ⁱ, Haibing Hu ^q,
 Hongbo Hu ⁱ, Q. Huang ^t, M. Iacovacci ^{f,e}, R. Iuppa ^{a,b},
 I. James ^{c,d}, H.Y. Jia ^t, Labaciren ^q, H.J. Li ^q, J.Y. Li ^s, X.X. Li ⁱ,
 B. Liberti ^b, G. Liguori ^{l,u}, C. Liu ⁱ, C.Q. Liu ^o, M.Y. Liu ^m,
 J. Liu ^o, H. Lu ⁱ, X.H. Ma ⁱ, G. Mancarella ^{g,h}, S.M. Mari ^{c,d},
 G. Marsella ^{h,v}, D. Martello ^{g,h}, S. Mastroianni ^e, X.R. Meng ^q,
 P. Montini ^{c,d}, C.C. Ning ^q, A. Pagliaro ^{n,w}, M. Panareo ^{h,v},
 L. Perrone ^{h,v}, P. Pistilli ^{c,d}, X.B. Qu ^s, E. Rossi ^e, F. Ruggieri ^d,
 L. Saggese ^{f,e}, P. Salvini ^l, R. Santonico ^{a,b}, P.R. Shen ⁱ,
 X.D. Sheng ⁱ, F. Shi ⁱ, C. Stanescu ^d, A. Surdo ^h, Y.H. Tan ⁱ,
 P. Vallania ^{j,k}, S. Vernetto ^{j,k}, C. Vigorito ^{j,r}, B. Wang ⁱ,
 H. Wang ⁱ, C.Y. Wu ⁱ, H.R. Wu ⁱ, B. Xu ^t, L. Xue ^s, Y.X. Yan ^m,
 Q.Y. Yang ^o, X.C. Yang ^o, A.F. Yuan ^q, M. Zha ⁱ, H.M. Zhang ⁱ,
 JiLong Zhang ⁱ, JianLi Zhang ⁱ, L. Zhang ^o, P. Zhang ^o,
 X.Y. Zhang ^s, Y. Zhang ⁱ, Zhaxisangzhu ^q, X.X. Zhou ^t,
 F.R. Zhu ⁱ, Q.Q. Zhu ⁱ, G. Zizzi ^{g,h}

^a*Dipartimento di Fisica dell'Università "Tor Vergata", via della Ricerca Scientifica 1, 00133 Roma, Italy*

^b*Istituto Nazionale di Fisica Nucleare, Sezione di Tor Vergata, via della Ricerca Scientifica 1, 00133 Roma, Italy*

^c*Dipartimento di Fisica dell'Università "Roma Tre", via della Vasca Navale 84,*

00146 Roma, Italy

^d*Istituto Nazionale di Fisica Nucleare, Sezione di Roma3, via della Vasca Navale 84, 00146 Roma, Italy*

^e*Istituto Nazionale di Fisica Nucleare, Sezione di Napoli, Complesso Universitario di Monte Sant'Angelo, via Cinthia, 80126 Napoli, Italy*

^f*Dipartimento di Fisica dell'Università di Napoli, Complesso Universitario di Monte Sant'Angelo, via Cinthia, 80126 Napoli, Italy*

^g*Dipartimento di Fisica dell'Università del Salento, via per Arnesano, 73100 Lecce, Italy*

^h*Istituto Nazionale di Fisica Nucleare, Sezione di Lecce, via per Arnesano, 73100 Lecce, Italy*

ⁱ*Key Laboratory of Particle Astrophysics, Institute of High Energy Physics, Chinese Academy of Science, P.O. Box 918, 100049 Beijing, P.R. China*

^j*Istituto Nazionale di Fisica Nucleare, Sezione di Torino, via P. Giuria 1, 10125 Torino, Italy*

^k*Istituto di Fisica dello Spazio Interplanetario dell'Istituto Nazionale di Astrofisica, corso Fiume 4, 10133 Torino, Italy*

^l*Istituto Nazionale di Fisica Nucleare, Sezione di Pavia, via Bassi 6, 27100 Pavia, Italy*

^m*Hebei Normal University, Shijiazhuang 050016, Hebei, China*

ⁿ*Istituto Nazionale di Fisica Nucleare, Sezione di Catania, Viale A. Doria 6, 95125 Catania, Italy*

^o*Yunnan University, 2 North Cuihu Rd, 650091 Kunming, Yunnan, P.R. China*

^p*Università degli Studi di Palermo, Dipartimento di Fisica e Tecnologie Relative, Viale delle Scienze, Edificio 18, 90128 Palermo, Italy*

^q*Tibet University, 850000 Lhasa, Xizang, P.R. China*

^r*Dipartimento di Fisica Generale dell'Università di Torino, via P. Giuria 1, 10125 Torino, Italy*

^s*Shandong University, 250100 Jinan, Shandong, P.R. China*

^t*South West Jiaotong University, 610031 Chengdu, Sichuan, P.R. China*

^u*Dipartimento di Fisica Nucleare e Teorica dell'Università di Pavia, via Bassi 6, 27100 Pavia, Italy*

^v*Dipartimento di Ingegneria dell'Innovazione, Università del Salento, 73100 Lecce, Italy*

^w*Istituto di Astrofisica Spaziale e Fisica Cosmica di Palermo - Istituto Nazionale di Astrofisica - via Ugo La Malfa 153 - 90146 Palermo - Italy*

^x*Istituto Nazionale di Fisica Nucleare - CNAF - viale Berti-Pichat 6/2 - 40127 Bologna - Italy*

Abstract

The ARGO-YBJ (Astrophysical Radiation Ground-based Observatory at YangBaJing) experiment is designed for very high energy γ -astronomy and cosmic ray researches. Due to the full coverage of a large area ($5600m^2$) with resistive plate chambers at a very high altitude (4300 m a.s.l.), the ARGO-YBJ detector is used to search for transient phenomena, such as Gamma-ray bursts (GRBs). Because the ARGO-YBJ detector has a large field of view (~ 2 sr) and is operated with a high duty cycle ($>90\%$), it is well suited for GRB surveying and can be operated in searches for high energy GRBs following alarms set by satellite-borne observations at lower energies. In this paper, the sensitivity of the ARGO-YBJ detector for GRB detection is estimated. Upper limits to fluence with 99% confidence level for 26 GRBs inside the field of view from June 2006 to January 2009 are set in the two energy ranges 10–100 GeV and 10 GeV–1 TeV.

Key words: Gamma ray bursts, Gamma-ray, Extensive air showers, Cosmic rays
PACS: 98.70.Rz, 95.85.Pw, 96.50.sd, 98.70.Sa

1 Introduction

Gamma-ray bursts (GRBs) are very strong gamma-ray photon emissions from cosmic unpredictable locations in a duration from milliseconds to tens of minutes. They are the most energetic form of energy released from a single object in such a short time. The total amount of light emitted in a GRB is usually a factor of hundreds brighter than a typical supernova. Using thousands of GRBs detected by satellite-based detectors, they have been thoroughly investigated in the keV–MeV energy range. They are isotropically distributed in the sky with a non-thermal origin. According to the time duration, GRBs are usually classified into long (>2 s) and short (<2 s) bursts. Since the first detection by the BeppoSAX satellite for GRB970228 [1], afterglows are observed after GRBs are discovered, and this enables the multi-wavelength investigation of GRBs from the optical band to X-rays. Redshift measurements show that GRBs occur at cosmological distances (the average redshift of GRBs observed by the Swift satellite is $z = 2.3$ [2]). Some short bursts come from inside old galaxies with little star formation, suggesting that they may be originated from mergers of binary neutron stars or black hole-neutron star systems [3]. Some long bursts are associated with supernovas and confirmed to be related to deaths of massive stars when central cores collapse to black holes [4].

* Corresponding author. Tel: +86 10 88236106; Fax: +86 10 88233086
Email address: chensz@ihep.ac.cn (S.Z. Chen).

High energy (HE) gamma-ray emissions from GRBs is also observed in several satellite-born experiments. Energetic Gamma-Ray Experiment Telescope (EGRET) detected several GRBs with photon energies ranging from 100 MeV to 18 GeV [5]. Both prompt and delayed emissions were detected and no high energy cutoff was found in the spectra. Most importantly, a distinct HE spectral component was evidently detected in GRB941017 [6]. Recently, Fermi Large Area Telescope (LAT) also detected GeV emissions from GRB080916C [7] and 081024B [8]. These observations at high energies can place important constraints on models of emission processes and on parameters of the environment surrounding the sources of bursts. Very high energy (VHE) emission up to \sim TeV is predicted by several models in both prompt and afterglow phases [9]. Emission at such high energies could result from electron Self-Synchrotron Compton (SSC) scattering in either internal or external, forward or reverse shocks. In such cases, a spectrum with double-peak shape extending into the VHE band is expected. Some models [10] also predict VHE emission due to decays of secondary π^0 mesons in neutron-rich outflows. Observations of VHE emission could play a role in discriminating between these models. The difficulty is that the absorption of the VHE photons by the Extragalactic Background Light (EBL), due to the pair production $\gamma + \gamma_{EBL} \rightarrow e^+ + e^-$, causes a substantial reduction of the VHE photon flux. This sets a high upper limit on the sensitivity of a detector used for GRB search in this energy range. The gamma-ray fluxes from these GRBs become too small to be detected from current satellite-based experiments due to their small sensitive areas, so only ground-based experiments have areas large enough for the detection.

Search for VHE emission from GRBs has been done by many ground-based experiments including extensive air shower arrays and Cherenkov telescopes. No conclusive detection has been made up to now, while some positive indications were reported. The Tibet $AS\gamma$ experiment found an indication of 10 TeV emission in a stacked analysis of 57 bursts [11]. The Milagro experiment reported evidence of emission above 650 GeV from GRB970417A with a chance probability of 1.5×10^{-3} [12]. Evidence of emission above 20 TeV from GRB920915C was reported about 1 min earlier than the GRB trigger time at 2.7σ level by the HEGRA AIROBICC array, but the position deviated of about 9° [13]. The muon detector GRAND found an excess during GRB971110 with a chance probability of 3×10^{-3} [14]. Due to limited field of view (FOV), Cherenkov telescopes, like MAGIC and HESS, can only be operated in follow-up mode and at least 40 s (usually minutes) are needed to sway the telescopes to point to the GRB. However, this sets very low upper limits to the photon fluences at energies around hundreds of GeV during the afterglow phase [15,16].

With a large FOV (~ 2 sr) and high duty cycle ($>90\%$), the ARGO-YBJ experiment, using a full coverage detector of Resistive Plate Chambers (RPCs) with area $5600m^2$, is well suited for GRB surveying. Following alarms by

satellite-borne observations of GRBs, the ARGO-YBJ detector is used to look for emission from them with a threshold of a few hundreds of GeV. No significant excess has been observed yet. In this paper, we place upper limits on the VHE emission fluences for the GRBs inside the FOV of the ARGO-YBJ detector. Two models with very different high energy cutoff are used. The detector performance is investigated using MC simulation. Based on this, the sensitivity of the ARGO-YBJ detector for GRB search at different time durations and incident zenith angles is presented in section 3. The processes of the data analysis and the method to search for VHE emission are described in section 4. The results are reported and discussed in section 5.

2 The ARGO-YBJ experiment

The ARGO-YBJ experiment, a collaboration among Chinese and Italian institutions, is designed for VHE γ -astronomy and cosmic ray observations and located in Tibet, China at an altitude of 4300m a.s.l. The detector consists of a single layer of RPCs, operated in streamer mode, with a modular configuration. The basic module is a cluster ($5.7 \times 7.6m^2$), composed of 12 RPCs ($2.850 \times 1.225m^2$ each). The RPCs are equipped with pick-up strips ($6.75 \times 61.80cm^2$) and the fast-OR signal of 8 strips constitutes the logical pixel (named pad) for triggering and timing purposes. Hundred and thirty clusters are installed to form a carpet of $5600m^2$ with an active area of $\sim 93\%$. This central carpet is surrounded by 23 additional clusters (“guard ring”) to improve the core location reconstruction. The total area of the array is $110 \times 100m^2$. More details about the detector and the RPC performance can be found elsewhere [17].

The RPC carpet is connected to two independent data acquisition systems, corresponding to the shower and scaler operation modes. With the scaler mode, each cluster of the ARGO-YBJ detector counts the rate of events that have total number of hits ≥ 1 , ≥ 2 , ≥ 3 and ≥ 4 every 0.5 s. Using the count rates, GRBs in the ARGO-YBJ detector FOV (zenith angle smaller than 45°) are investigated without direction information [18].

In shower mode, the ARGO-YBJ detector is operated by requiring at least 20 particles within 420 ns on the entire carpet detector. The high granularity of the apparatus permits a detailed spatial-temporal reconstruction of the shower front. The temporal information is the arrival time of particles measured by Time to Digital Converters (TDCs) with a resolution of approximately 1.8 ns. This results in an angular resolution of 0.2° for showers with energy above 10 TeV and 2.5° at approximately 100 GeV [19]. In order to calibrate the 18,360 TDC channels, an off-line method [20] is developed using cosmic ray showers. The calibration precision is 0.4 ns by using 24 h of data and the calibration

result is updated every month [21].

The central 130 clusters began taking data in June 2006, and the "guard ring" was merged into the DAQ stream in November 2007. The trigger rate is ~ 3600 Hz and the average duty cycle is higher than 90%.

3 Simulation and sensitivity

The effective area of the ARGO-YBJ experiment for detecting gamma-ray showers is estimated by using a full Monte Carlo simulation driven by CORSIKA 6.502 [22] and GEANT3-based code ARGO-G [23]. Five zenith angles ($\theta = 0^\circ, 10^\circ, 20^\circ, 30^\circ$ and 40°) are chosen in the simulation and the sampling area is $300 \times 300 m^2$ around the carpet center. The threshold multiplicity of hits (N_{hit}) which triggers ARGO-YBJ is 20. The effective areas for this threshold at the three zenith angles $\theta = 0^\circ, 20^\circ$ and 40° are shown in Fig.1.

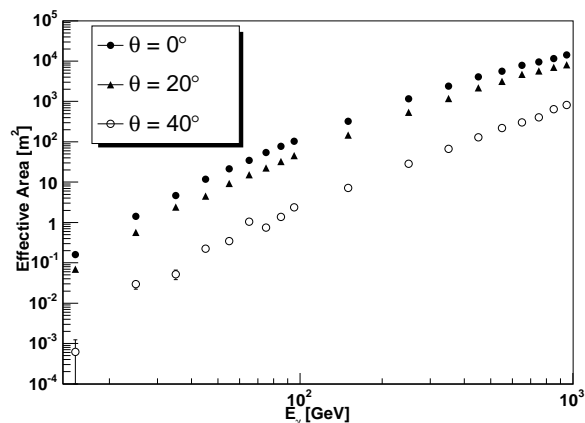


Fig. 1. Effective areas of ARGO-YBJ for gamma rays with $N_{hit} \geq 20$ as a function of the energy for the three zenith angles $\theta = 0^\circ, 20^\circ$ and 40° .

In order to avoid strong absorption of VHE photons by the EBL, two models of GRB emission with sharp cutoff of their spectra at 100 GeV and 1 TeV are investigated. Since the multiplicity of hits N_{hit} in an event is related to the shower primary energy, the optimization of the ARGO-YBJ sensitivity can be done by choosing a corresponding cutoff on N_{hit} . As results of the optimization, ranges of N_{hit} are found corresponding to the two E_{cut} models as reported in Table 1. Given the ranges of N_{hit} , the corresponding optimal opening angle radii ϕ_{70} , inside which 70% of the signal events is included, are reported in Table 1. This result is almost independent of zenith angle. After using the event selection listed in Table 1, the average effective areas $\langle A \rangle$ over the energy ranges from 10 GeV to 100 GeV and from 10 GeV to 1

TeV with a differential spectral index -2.0 (this assumption is used in all the following analyses) are calculated as functions of the zenith angle θ . They fit a functional form $\langle A \rangle = A_0 \cos^n \theta$, where $A_0 = 4.36 \pm 0.04 m^2$ and $119.3 \pm 0.8 m^2$ are the average effective areas at $\theta = 0^\circ$, with the parameter $n = 14.26 \pm 0.11$ and 10.56 ± 0.13 for the two energy ranges, respectively (see Fig.2); with these functions the average effective areas at any zenith may be obtained. At $\theta = 20^\circ$, the effective area of the ARGO-YBJ detector is about $1.8 m^2$ above 10 GeV if the cutoff energy E_{cut} of the GRB spectrum is chosen as 100 GeV. On the other hand, it is $64.3 m^2$ if $E_{cut} = 1000$ GeV.

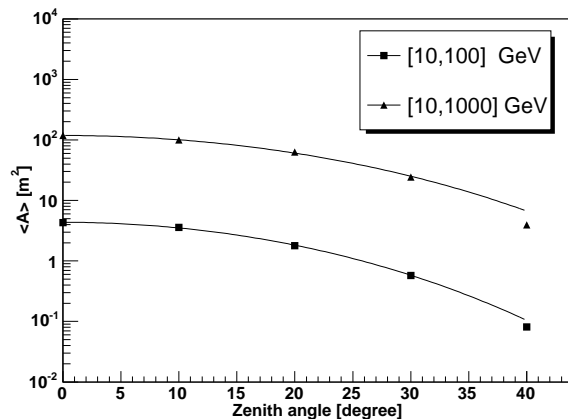


Fig. 2. The average effective area in two energy ranges after using the event cut listed in Table 1 as a function of zenith angles. The lines are the fitting result using the function $A_0 \cos^n \theta$.

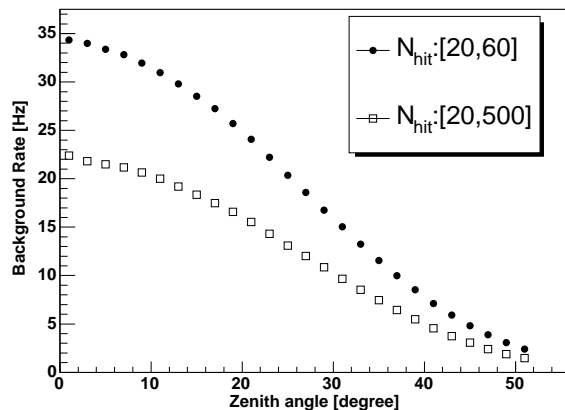


Fig. 3. The background rate detected in two different data selection conditions listed in Table 1 as a function of the incident zenith angle. This figure was made with data taken from one hour before to one hour after the GRB080903 trigger time, and every point stands for the average value from different azimuth angles.

Using measured cosmic ray data, the background event rate (see Fig.3) is es-

Table 1

N_{hit} ranges and corresponding angular window sizes for gamma rays.

E_{cut} (GeV)	N_{hit}	ϕ_{70} ($^{\circ}$)
100	20-60	3.8
1000	20-500	2.6

timated according to the selected N_{hit} ranges reported in Table 1. Combining this with the effective areas shown in Fig.2, the minimum detectable fluences for GRBs requiring a 5σ excess are estimated and shown in Fig.4. The sensitivity worsens with the increase of the zenith angle. The GRB time duration in this figure is fixed at $T = 12$ s and the fluence scales with $T^{1/2}$. We find that the ARGO-YBJ detector has a sensitivity of 10^{-5} erg/cm^2 in the energy range [10,1000] GeV for GRBs with a duration of 12 s at $\theta = 20^{\circ}$.

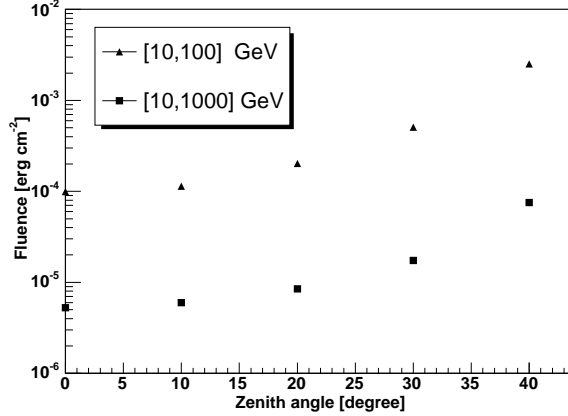


Fig. 4. The 5σ minimum detectable fluences for GRBs with a duration 12 s in the two energy ranges [10,100] GeV and [10,1000] GeV for different incident zenith angles.

4 Data analysis

In an angular window surrounding the GRB with the aperture given in Table 1, the N_{on} events that fall in N_{hit} ranges are taken as on-source. Among these, the contribution from the cosmic ray background, N_b , is estimated by integrating all the events over 2 h around the GRB trigger time, referred as “direct integral method” in the literature [24]. The significance of any excess in the on-source events is calculated using Eq. (17) of Li and Ma [25].

As widely discussed, the acceleration mechanism for VHE emission could be different from that at low energies, so that it could be on a different time scale. Even if the duration of every burst detected by satellite is known, the duration

Table 2

The absorption factor $K(z)$ due to the EBL is $K(z) = \int A(E)(dN/dE)dE / \int A(E)(dN/dE)e^{-\tau_{EBL}} dE$.

Energy (GeV)	redshift	$\theta = 0^\circ$	$\theta = 10^\circ$	$\theta = 20^\circ$	$\theta = 30^\circ$	$\theta = 40^\circ$
10-100	0.5	1.08	1.08	1.08	1.08	1.09
	1.0	1.39	1.39	1.39	1.39	1.40
	2.3	3.39	3.39	3.40	3.40	3.54
10-1000	0.1	1.60	1.61	1.66	1.72	1.75
	0.5	7.92	8.02	9.27	11.13	11.66
	1.0	25.71	26.05	31.59	39.19	41.84
	2.3	116.5	118.7	147.6	181.3	209.2

of VHE emission is still unknown. It is believed that (a) the most probable emission time is still in the prompt phase; (b) the emission may be delayed even by hours, like in the case of the 18 GeV photon in GRB940217, detected 1.5 h after the prompt emission [26]; (c) the high energy emission could be produced earlier according to some models [27]. The GRB counterpart is first searched in a window T_{90} , which is defined as the time in which 90% of the GRB photons is released. If no signal is found, we continue the search from 1 h before to 1 h after the GRB. Time intervals of 1 s, 6 s, 12 s, 24 s, 48 s and 96 s are used in this search with steps 1 s, 2 s, 3 s, 6 s, 12 s and 24 s, respectively. If no signal is found, we set an upper limit to the fluence in T_{90} .

Given the observed N_{on} and the expected background N_b in T_{90} , the upper limits for the number of events, N_{UL} , with confidence level of 99% is calculated with Helene's method (Eq. (10) in [28]). Using the effective area and assuming a differential power law photon spectrum, the upper limit to the fluence of a GRB in the VHE range is obtained. Guided by the average spectrum of the four bright bursts observed by EGRET, where a power law index of -1.95 ± 0.25 was found over the energy range from 30 MeV to 10 GeV [5], an energy spectrum $dN/dE = CE^{-2}$ is assumed. At first, the normalization constant C is calculated by solving the equation $N_{UL} = \int A(E)(dN/dE)e^{-\tau_{EBL}} dE$. Then the total fluences can be obtained by integrating $\int E(dN/dE)dE$ from 10 GeV to 100 GeV and to 1 TeV. The τ_{EBL} is the optical depth due to the EBL absorption, and the optical depths predicted by A. Franceschini [29] are used in this work. The absorption factor, which is defined as the ratio $K(z) = \int A(E)(dN/dE)dE / \int A(E)(dN/dE)e^{-\tau_{EBL}} dE$, for GRBs at redshift $z = 0.1, 0.5, 1.0$ and 2.3 are listed in Table 2. According to these results, the EBL effect for gamma-rays below 100 GeV is negligible, however, it could be substantial for farther GRBs in the range [10,1000] GeV. With the absorption factor $K(z)$ and the average effective area $\langle A \rangle$ shown in Fig.2, the parameter C can be directly calculated by solving the equation $N_{UL}/(K(z)\langle A \rangle) = \int (dN/dE)dE$.

5 Results and discussion

The data used in this work were collected by the ARGO-YBJ experiment in the periods July 2006–July 2007 and November 2007–January 2009. Twenty-six GRBs detected by satellites were within the FOV of the detector array while it was on. Angular resolution, pointing accuracy and stability of the ARGO-YBJ detector were thoroughly tested by measuring the Moon shadow in cosmic rays over all observational periods [30]. The Crab Nebula and flares of Mrk421 in years 2006 and 2008 were successfully detected [31].

No significant excess was observed for any of the 26 GRBs, neither as prompt nor prior/delayed emission (see Fig.5). Upper limits to fluences in the VHE range are listed in Table 3. The upper limits for the 6 GRBs with redshift information have been corrected for EBL absorption, while the others can be easily corrected using the factors listed in Table 2 assuming $z = 0.1, 0.5, 1.0$ and 2.3 . The fluences in keV bands measured by the satellite experiments are also listed in Table 3.

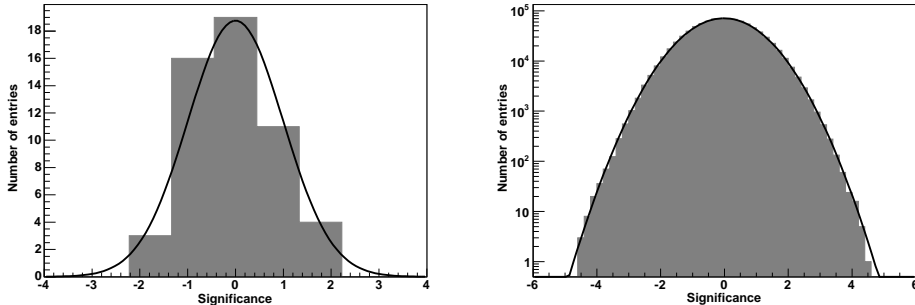


Fig. 5. Left: Distribution of the statistical significance of the 26 GRBs with data available during their prompt phase using both events selections of Table 1. Right: Distribution of the statistical significance derived from two hours of observations around the 26 GRBs analysed with different time durations. The solid lines are normal Gaussian functions for given comparison.

It is known that GRB spectra can be well fitted with a Band function with a break at energy E_0 mostly between 100 keV and 1 MeV, and the average index α below the break is ~ -1 and the average index β above the break is ~ -2.3 [32]. Most GRBs observed by Swift do not have such a clear spectral structure with a break since its effective energy range is often lower than the break energy. GRB060805B was detected by the Inter Planetary Network (IPN) from 30 keV to 10 MeV and the result of fitting the data with the Band function ($\alpha = -0.66$, $\beta = -2.52$ and $E_0 = 240$ keV) is shown in Fig.6 (solid line). If this GRB spectrum extends to TeV energies only following the Band function, it will be compatible with the upper limits obtained by ARGO-YBJ.

Table 3

List of GRBs in the FOV ($\theta < 45^\circ$) of ARGO-YBJ and 99% C.L. fluence upper limits

GRB	Satellite	Redshift	T_{90} (s)	$\theta(^{\circ})$	keV fluence (keV range)	10–100 GeV <i>erg cm⁻²</i>	10–1000 GeV <i>erg cm⁻²</i>
060714	Swift	2.71	115	42.8	2.9E-6 (15-150)	2.10E-2	3.11E-2
060805B	IPN	...	8	29.1	1.1E-4 (30-10000)	1.29E-4	5.08E-6
060807	Swift	...	43.3	12.4	8.5E-7 (15-150)	7.32E-5	4.23E-6
060927	Swift	5.47	22.6	31.6	1.2E-6 (15-150)	6.63E-3	1.56E-2
061028	Swift	...	106	42.5	9.7E-7 (15-150)	6.23E-3	1.08E-4
061110A	Swift	0.76	41	37.3	1.1E-6 (15-150)	1.23E-3	5.32E-4
061122	Integral	...	18	33.5	2.3E-5 (20-2000)	4.27E-4	8.45E-6
070306	Swift	1.50	210	19.9	5.5E-6 (15-150)	5.86E-4	9.63E-4
070531	Swift	...	44	44.3	1.1E-6 (15-150)	3.09E-3	7.82E-5
070615	Integral	...	30	37.6	...	1.42E-3	3.93E-5
071112C	Swift	0.82	15	22.1	3.0E-6 (15-150)	2.02E-4	1.04E-4
080207	Swift	...	340	27.7	6.1E-6 (15-150)	8.95E-4	3.31E-5
080324	Integral	...	13.6	14.6	...	8.52E-5	5.19E-6
080328	Swift	...	90.6	37.2	9.4E-6 (15-150)	1.60E-3	4.79E-5
080602	Swift	...	74	42.0	3.2E-6(15-150)	3.31E-3	1.32E-4
080613B	Swift	...	105	39.2	5.8E-6(15-150)	2.49E-3	7.32E-5
080726	AGILE	...	125	36.7	...	2.38E-3	5.21E-5
080727C	Swift	...	79.7	34.5	5.3E-6(15-150)	8.15E-4	3.18E-5
080822B	Swift	...	64	40.4	1.7E-7(15-150)	2.55e-3	9.46E-5
080903	Swift	...	66	21.5	1.5E-6(15-150)	1.73e-4	7.03e-6
081025	Swift	...	23	30.5	1.9E-6(15-150)	3.75E-4	1.56E-5
081028	Swift	3.04	250	29.9	3.7E-6(15-150)	7.72E-3	1.25E-2
081105	Swift	...	10	36.7	...	4.09E-4	1.30E-5
081128	Swift	...	101.7	31.7	2.5E-6(15-150)	6.21E-4	2.05E-5
090107	Swift	...	12.2	40.1	2.3E-7(15-150)	7.38E-4	3.21E-5
090118	Swift	...	16	13.4	4.0E-7(15-150)	6.68E-5	3.68E-6

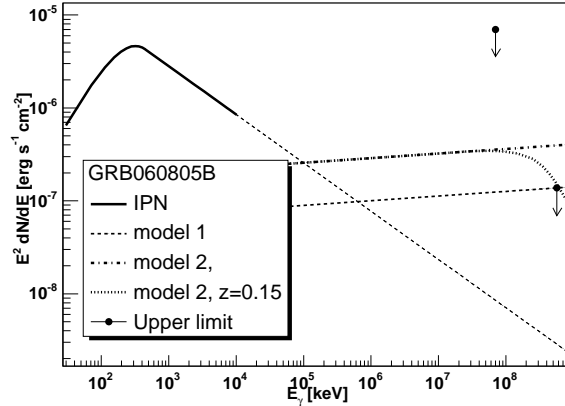


Fig. 6. The spectrum of GRB060805B and the upper limits obtained by ARGO-YBJ. The solid line is the result of fitting the IPN data with the Band function and the dotted line is a simple extrapolation. The upper limits are located at the mean energies of gamma ray events. For details about model 1 and model 2 see text.

However, the spectrum might not extend with a simple power law ($\beta = -2.52$) above 100 MeV. It might turn to $\beta = -1.95$ like the four bright bursts detected by EGRET observations [5]. If EBL absorption is negligible, the limit found by this work implies that the transition energy should be above 620 MeV (see model 1 in Fig.6). The other possibility is that if the transition energy is 100 MeV for this burst, the source should be farther than $z = 0.15$ (see model 2 in Fig.6). In addition, if the SSC mechanism used by Finke et al. ([33]) to interpret the spectrum of GRB 940217 also works on GRB060805B, the limit found by this work will provide a strong constraint.

In conclusion, we have investigated 26 gamma-ray bursts in the field of view of ARGO-YBJ in about two years in the GeV–TeV energy range searching for prompt, delayed or prior emission. Since no significant excess is found, we have set upper limits to fluences for most of those bursts.

6 Acknowledgements

This work is supported in China by the National Natural Science Foundation of China (NSFC) under the grant 10120130794, the Chinese Ministry of Science and Technology, the Chinese Academy of Sciences (CAS), the Key Laboratory of Particle Astrophysics, Institute of High Energy Physics (IHEP), and in Italy by the Istituto Nazionale di Fisica Nucleare (INFN). M. Dattoli thanks the National Institute of Astrophysics of Italy (INAF) for partly supporting her activity in this work.

References

- [1] E. Costa et al., *Nature* 387 (1997) 783.
- [2] N. Gehrels, AIP Conf. Proc., *Gamma-Ray Bursts 2007 (Santa Fe)*:3.
- [3] J.S. Bloom et al., *Astrophys. J.* 638 (2006) 354.
- [4] A.I. MacFadyen, S.E. Woosley, *Astrophys. J.* 524 (1999) 262.
- [5] B.L. Dingus, AIP Conf. Proc. 558 (2001) 383.
- [6] M.M. Gonzalez et al., *Nature* 424 (2003) 749.
- [7] H. Tajima , J. Bregeon , J. Chiang et al., (2008) GCN #8246.
- [8] N. Omodei et al., (2008) GCN #8407.
- [9] P. Mészáros et al., *Rep. Prog. Phys.* 69 (2006) 2259.
- [10] J. Razzaque et al., *Astrophys. J.* 650 (2006) 998.
- [11] M. Amenomori et al., *Astron.& Astrophys.* 311 (1996) 919.
- [12] R. Atkins et al., *Astrophys. J.* 533 (2000) L119.
- [13] L. Padilla et al., *Astron.& Astrophys.* 337 (1998) 43.
- [14] J. Poirier et al., *Phys. Rev. D* 67 (2003) 042001.
- [15] J. Albert et al., *Astrophys. J.* 667 (2007) 358.
- [16] F. Aharonian et al., *Astron.& Astrophys.* 495 (2009) 505.
- [17] G. Aielli et al., *Nucl. Instr. and Meth. A* 562 (2006) 92.
- [18] G. Aielli et al., *Astropart. Phys.* 30 (2008) 85.
- [19] G. Di Sciascio et al., *30th ICRC 4* (2007) 123.
- [20] H.H He et al., *Astropart. Phys.* 27 (2007) 528.
- [21] G. Aielli et al., *Astropart. Phys.* 30 (2009) 287.
- [22] J.N. Capdevielle et al., *KfK Report* (1992) No.4998.
- [23] <http://argo.le.infn.it/analysis/argog/>.
- [24] R. Fleysher et al., *Astrophys. J.* 603 (2004) 355.
- [25] T.P. Li, Y.Q. Ma, *Astrophys. J.* 272 (1983) 317.
- [26] K. Hurley et al., *Nature* 372 (1994) 652.
- [27] X.H. Ma et al., *HEP & NP* 27 (2003) 973 (in Chinese).
- [28] O. Helene, *Nucl. Instr. and Meth.* 212 (1983) 319.

- [29] A. Franceschini et al., *A & A* 487 (2008) 837.
- [30] B. Wang et al., 30th ICRC 4 (2007) 107.
- [31] G. D'Alí Staiti et al., *Nucl. Instr. and Meth. A* 588 (2008) 7.
- [32] R.D. Preece et al., *Astrophys. J. S.* 126 (2000) 19.
- [33] J.D. Finke et al., arXiv:0802.1537v1 [astro-ph].